Top. Meteoro. Oceanog. 9 (2)88-103, 2002

Some Characteristics of the Annual Precipitation Cycle in Central America and their Relationships with its Surrounding Tropical Oceans

ERIC J. ALFARO[1]

School of Physics (DFAOP), Center for Research in Geophysical Sciences (CIGEFI) and Center for Research in Marine Sciences and Limnology (CIMAR), University of Costa Rica, 2060-Ciudad Universitaria Rodrigo Facio, San José, Costa Rica

(Recibido 6 de febrero 2002, aceptado 24 de mayo de 2002)

ABSTRACT

Using 94 daily rain gauge stations, the mean dominant annual cycles in the Central American region were calculated using empirical orthogonal functions analysis. This allowed determination of some important aspects of this cycle such as the start and end of the rainy season and the mid summer drought. Some latitudinal variations were found in these variables. The region was dominated by one mean annual cycle that captured 72% of the variance. This cycle implied mainly a combination of systems and parameters that involved the latitudinal migration of the ITCZ, the seasonal variation of solar radiation that influences latent heat flux, and the low level wind and its interaction with local orography. The second in importance annual cycle explains only the 8% of the variance and dominated in stations located over the Caribbean Coast of Honduras, Costa Rica and Panama. The precipitation in Central America shows different relationships with the tropical Atlantic and Pacific oceans in the interannual and decadal scales. In the interannual scale, the wettest (driest) years in the region were dominated in general by warmer (colder) sea surface temperature in the tropical Atlantic compared with the eastern tropical Pacific. While in the decadal scale, the precipitation shows positive correlations with both tropical ocean regions.

Introduction

Most of the Central America's rainfall studies have pointed out that, although this region is practically under the influence of maritime air masses, the local and seasonal variations of precipitation are surprisingly high and some of this variability can be attributed to seasonal variations in the lower winds associated with the dynamics of the Central American atmosphere and their interaction with the local topography (Portig, 1976; Waylen *et al.*, 1996).

As an introduction to the problem, the two rainfall dominant mean annual cycles were calculated using Empirical Orthogonal Functions (EOFs) analysis of 337 monthly grid points over or very close to land in Central America (Fig. 1). Fig. 1a shows the dominant regime and explains 86.7% of the total variance. It shows two rainfall maxima, the first one in June and the second largest one in September. Between these two maxima there is a relative minimum in July-August called *veranillo, canícula* or Mid Summer Drought (MSD) (Magaña *et al.*, 1999). The dry season occurs in winter and early spring and is more intense in the Pacific slope of the isthmus. Fig. 1b is the second regime of importance and captures only 8.2% of the total variance. This regime is found near the Caribbean coast of Honduras and Costa Rica (Fig. 1c). It also has two maxima but these occur in the months of July and November, with the second being wetter than the first one, and two minima in March and September, with the first one drier than the second one.

The secular trend of the region is presented in Fig. 2a, taking as the average of the precipitation anomalies (PCPA) time series of the grid points in the Fig 1c. There is no clear or significant trend in the region because the signs of this parameter in the region do not show complete spatial coherence (Fig. 2b).

Although grid data sets similar to the one presented in Figs. 1 and 2 are, in general, useful to study the influence of climate variability phenomena of great spatial and time scale over the region, there are two major problems associated to the use of this kind of data sets. First, there is a great spatial variability in the region and the grid process could combine different annual cycles in the same grid point. Second, it is not possible to define some important aspects of the annual cycle, such the Start or End date (SD and ED, respectively) of the rainy season or the MSD, because their associated time scale is shorter

[1] Dirección postal: Escuela de Física, Universidad de Costa Rica, 2060 Ciudad Universitaria Rodrigo Facio, San José, Costa Rica.
Correo electrónico: ejalfaro@cariari.ucr.ac.cr,

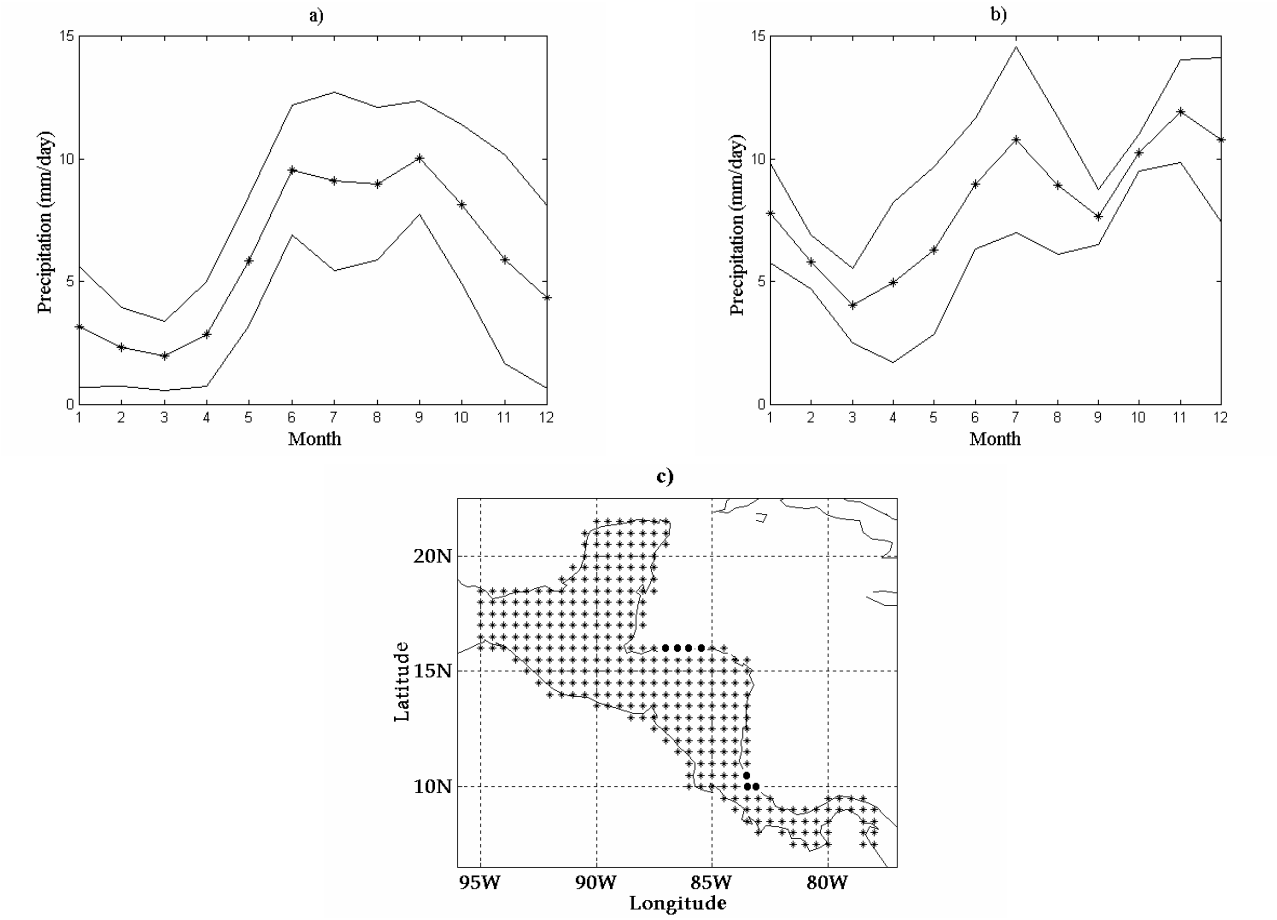

Fig. 1. Lines with asterisks are the a) First and b) Second rainfall dominant annual cycle patterns, using EOF analysis, of 337 grid points over or very close to land in Central America, covering 78.0-95.0°W, 7.5-21.5°N. Bands are given for one standard deviation (solid lines). These data were compiled by the Centro de Ciencias de la Atmósfera in the UNAM, Mexico. They used data from gauge stations, satellite outputs and numerical models to produce the grids, which are 0.5° latitude x 0.5° longitude. The time period covers from January 1958 to August 1999. The sources of this data are described in Magaña *et al.* (1999). c) Spatial location of grid points, asterisks (solid circles) are

than a month (Enfield and Alfaro, 1999; Magaña *et al*., 1999).

These aspects of the rainy season are very important for planning in key sectors such as agriculture and power generation and have been the focus of several studies in the Americas. Magaña *et al*. (1999) used biweekly climatic data in a 1° x 1° resolution, in order to define the spatial resolution of the MSD in Central America. They postulated a hypothesis that involved positive and negative feedbacks between the sea surface temperatures (SSTs) of the Northeast Pacific Warm Pool (Wang and Enfield, 2001) and the overlaying atmosphere that manage the MSD. Also, Alfaro and Cid (1999a, b), Alfaro *et al.* (1998) and Enfield and Alfaro (1999) used stations with daily records over Central America and concluded that SD and ED in this region are related to interannual variability of the SST in the tropical north Atlantic (TNA) and the eastern tropical Pacific. More recently, Cortez (2000) used a different approach and calculated the climatic SD, MSD and ED based in Out-going Long wave Radiation (OLR) data over Central America and Southern Mexico and pointed out that the intensity of the low level wind over the region is consistent with the onset and evolution of the rainy season.

In a couple of recent papers, Enfield and Mestas-Nuñez (1999) and Mestas-Nuñez and Enfield (1999), have identified the three and six lead modes for non-ENSO global 1856-1991 SST anomalies (SSTAs), using unrotated and rotated complex empirical functions respectively. As these authors explain, the unrotated modes efficiently describe the global variance of the data but they generally do not represent a large fraction of the variance in any given region, therefore they applied an orthogonal rotation to the non-ENSO EOFs to investigate the presence of regionalized centers of variability. These modes are related to different atmospheric forcing and tropospheric patterns that could be associated with the long-term climate variability in the Central American region (Goldenberg *et al.*, 2001; Mestas-Nuñez and Enfield, 2001).

The main objective of this study is to calculate the climatic values for the SD, ED and MSD of the rainy season, using daily rainfall gauge stations records in Central America, associated with the dominant mean

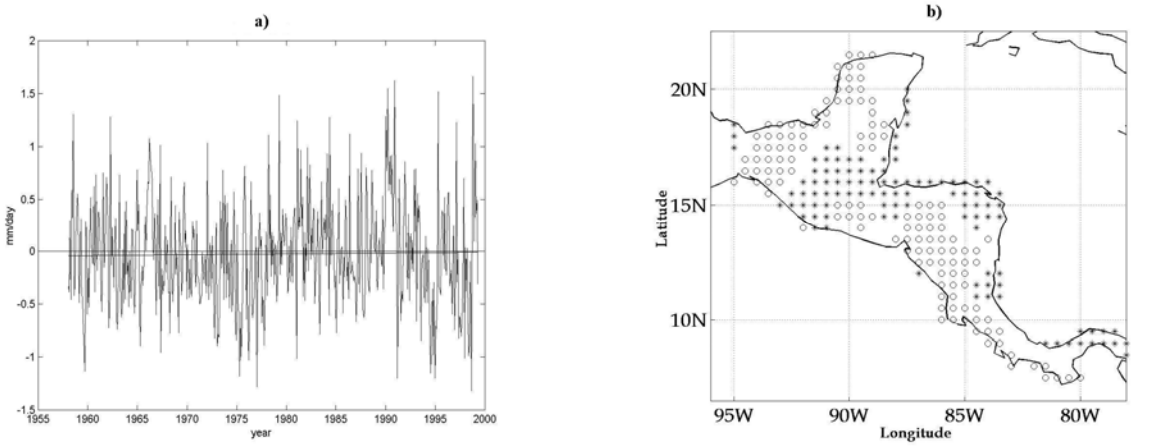

Fig. 2. a) Mean precipitation anomalies time series of the grid points show in Fig. 1. The solid line is its positive linear trend that is not statistically significant at the 95% level. b) Open circles (asterisks) are negative (positive) trends for the precipitation anomalies time series of the grid points showed in Fig. 1. These values are statistically significant at the 95% level.

annual cycle pattern. Also, considering the results of the studies cited previously, a second objective is to associate some of these structures of the precipitation annual cycle with the interannual variability of the TNA and the eastern Pacific oceans, and also to investigate the correlation between the leading EOF modes of the PCPAs in the isthmus and the SSTAs modes described before in the decadal scale.

2. Data sets and methods

In this study, daily records of 94 rain gauge stations in Central America were used. Their geographic locations are shown in Fig. 3. This complements previous regional studies (e.g. Alfaro and Cid, 1999b) using a better geographical coverage. Only records with at least 10 years of data were analyzed. These data were transformed to pentad or 5-day accumulated rainfall records, which reduce the noise and give 73 pentads for a year. After that, pentad's climatologies were calculated, to produce a mean annual cycle of 73 values by station and were used EOF analysis to identify the dominant mean annual cycles in the region (Giannini *et al.,* 2000).

For any mean annual cycle of any station, the SD was calculated according to the methodology used by Enfield and Alfaro (1999). They suggested that the SD is already established if, checking an individual year from pentad 1 to 73, a pentad with 25 mm or more rainfall is found and at least one of the two succeeding pentads exceeds the same threshold, and the two pentads surrounding or following the latter exceed a trace as daily average. ED establishment is similar, but mean annual cycles are checked in reverse. Marengo *et al.* (2001) used a similar methodology for the Amazon region. MDSs were defined as the lowest minimum of the climatic annual cycle between the two rainfall maxima of the rainy season. More formal and extended definitions of the SD, MSD and ED can be found in Alfaro and Cid (1999b) and Magaña *et al*. (1999).

The NCEP/NCAR Reanalysis Monthly Data Set from 1982 to 1994 were used to create climatic values of latent heat flux (LHF in Wm^{-2}), Out-going Long wave Radiation (OLR in Wm^{-2}) and specific humidity divergence ($\tilde{\mathbf{N}} \times (q\,\mathbf{V})$, in s^{-1}); over 75-95° W, 5-20° N, where q is the specific humidity in kg/kg and **V** is the surface velocity vector in ms^{-1}. The fields associated to these parameters were calculated for January (dry season), May (transition from dry to rainy season), June (first rainfall maximum month), July (MSD month), September (second rainfall maximum month), and November (transition from rainy to dry season) (Fig. 1a). In spite that these data have a relatively coarse spatial resolution, specially when considering the Central American isthmus is less than 2.5 degrees wide and the effects of topography are crucial in explaining the annual cycle of precipitation, they were used as a rough guide to explain some of the large scale spatial features that could influence the precipitation in the region.

In order to evaluate the association of anomalous wet and dry years in the Central American precipitation with the interannual variability of the Tropical Atlantic and Pacific oceans, four parts of the annual cycle with common characteristics were used (Fig. 4a). The first part (FiP), with a positive trend and associated to the SD, is between Julian days 97 and 153. The second part (SP) is associated with the MSD, and is between Julian days 154 and 245. The third part (TP), with a negative trend and associated with the ED, is between Julian days 246 and 357. Finally the fourth part (FoP) is associated with the dry season, and is between Julian days 358 and 96.

Stations with at least 20 years of complete daily records during any of the part of the rainy season described above were identified. This was done between the years 1950-1994 because it was the time period in which more stations had complete daily records (see for example Fig. 5). For every part of the annual cycle, these years where ranked and divided in five categories according to three variables: accumulates, days with precipitation and consecutive days with precipitation, except for the dry season in which only accumulates were

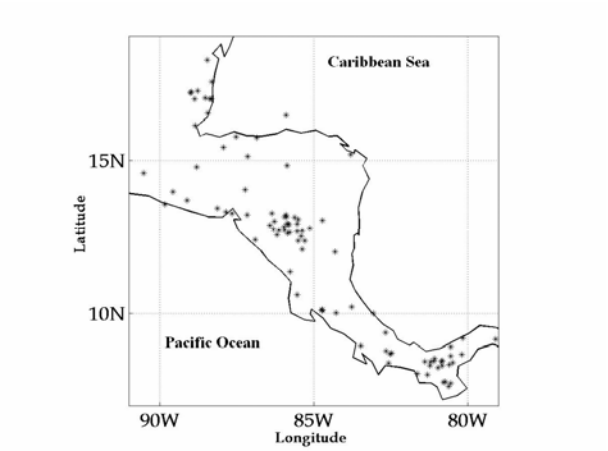

Fig. 3. Asterisks represent the geographic location of the gauge stations used in this study.

used because the last two variables described do not separate classes well. The working group that participates in the Central American Climatic Forums in Central America suggested these three variables to study the impact of dry and wet years over the region. Frequency histograms were prepared for all the years identified in the first (driest years) and the fifth (wettest years) categories in all the stations. For the four parts of the rainy season described, the selection of the wettest and driest years with the greatest impact over the region were based in the average histogram of the three variables described before. In spite that in general correlations between these variables are positive (see for example Fig. 6), the rank of these years could be different if they are based in just one of the described variables, as Table 1 shows for the SP.

As a second step, anomaly seasonal values of Niño 3.4 and TNA SSTA indices were prepared for April-May, June-July-August, September-October-November-December and January-February-March, that match approximately parts of the precipitation annual cycle described. These seasonal values were calculated between 1856 and 1999 (144 values). These values where ranked and divided in five categories with the coldest values in the first category and the warmest values in the fifth category. The difference in the rank position of seasonal SSTA indices was calculated for the years identified in the different parts of the rainy season. This categorical approach was preferred mainly because of the influence, in terms of magnitude, of any SST anomaly in the Pacific, and was also compared with one in the Atlantic, a non-clear issue.

Finally, the data used in the Figs. 1 and 2 were low-filtered by a triangular moving average of 121 points (Soley, 1994) and their non-rotated EOFs were correlated with the first three unrotated global SSTA modes used in Enfield and Mestas-Nuñez (1999) and the first six rotated global SSTA modes of Mestas-Nuñez and Enfield (1999) in order to identify some possible relationships between oceanic climatic variations and the PCPA in Central America in the decadal scale.

3. Results and Discussion

3.1 Annual Cycle

As in Fig. 1a, the pentad mean annual cycle in the region is described by one dominant mode, using EOFs analysis, explaining 72.0% of the variance (Fig. 4a). The precipitation mean annual accumulated by this regime is 2125 mm, with a range, given by one standard deviation

Table 1. First eight wettest and driest years for the SP of the precipitation annual cycle according to accumulates, days with precipitation and consecutive days with precipitation.

	Wet Years			Dry Years		
Rank	**Acumulates**	**Days with Precipitation**	**Consecutive days with Precipitation**	**Acumulates**	**Days with Precipitation**	**Consecutive days with Precipitation**
1	1988	1988	1988	1982	1982	1982
2	1964	1964	1964	1972	1991	1986
3	1981	1969	1973	1965	1986	1991
4	1973	1966	1969	1976	1976	1976
5	1969	1973	1968	1986	1972	1990
6	1966	1981	1966	1991	1965	1965
7	1970	1968	1960	1957	1975	1972
8	1984	1960	1962	1990	1990	1953

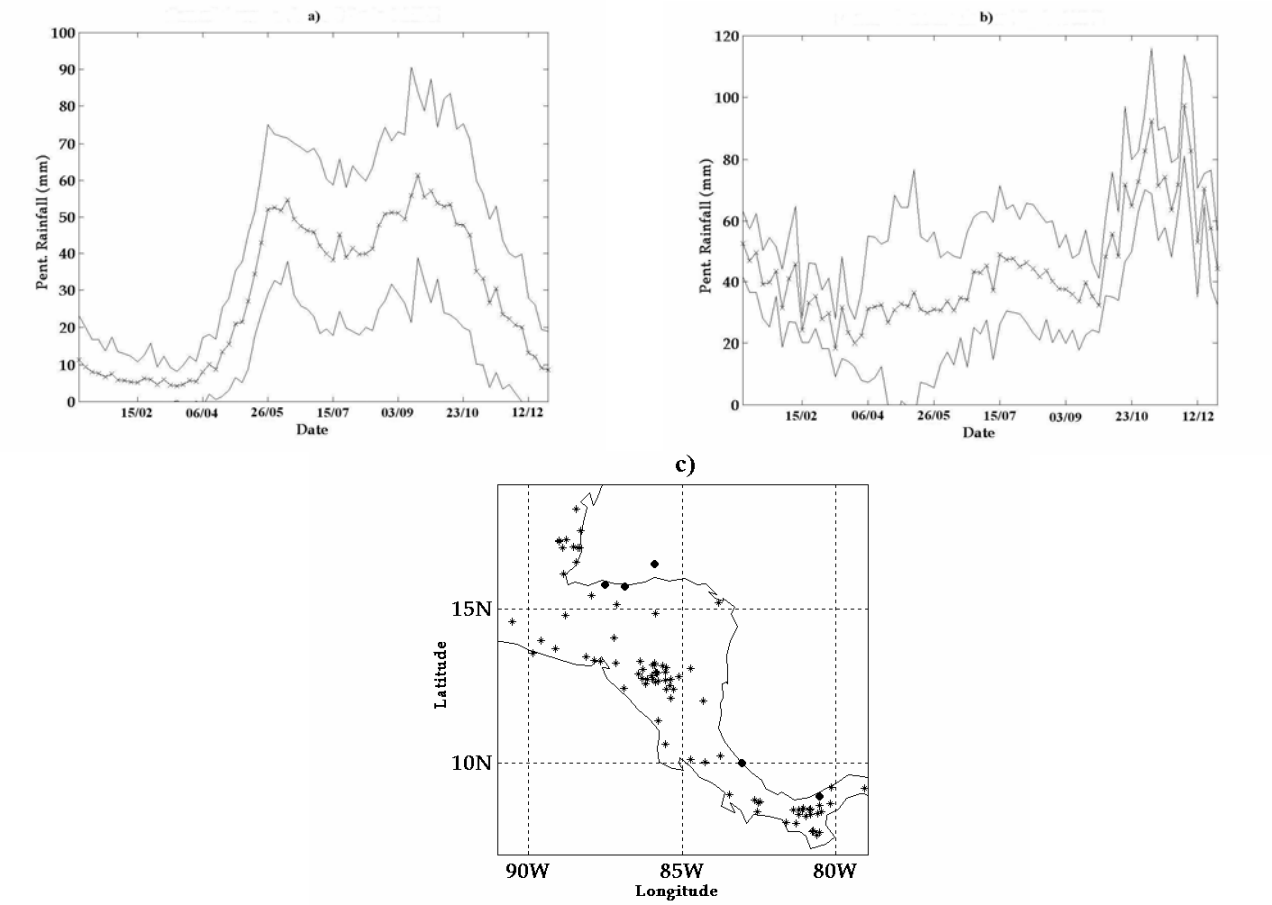

Fig. 4. Lines with asterisks are the a) First and b) Second pentad rainfall dominant annual cycle patterns, using EOFs analysis, of the 94 gauge stations used. Bands are given for one standard deviation (solid lines). c) Asterisks (solid circles) are points in which the first (second) mode dominates.

(solid lines in Fig. 4a), of 896-3354 mm. The results of Figs. 1a and 4a agree in general with the first principal component of the annual cycle presented by Giannini *et al.* (2000), but using a more extended region in the Caribbean basin. This regime has a dry season that accumulates only 16.4% of the annual total between the middle of November and the end of May. This season is characterized by strong trade winds (Fig. 7) and high values of total radiation (R_t, direct plus diffuse radiation) and sunshine hours in low troposphere levels (Figs. 8a and c), despite the fact that the radiation in at top of the atmosphere (R^{TA}) is at minimum. According to Cortez (2000), there is no evidence of deep convection because OLR values are greater than 240 Wm^{-2} and there is also poor humidity convergence over almost all the isthmus excepting the Southeast (Figs. 9a and 10a, respectively).

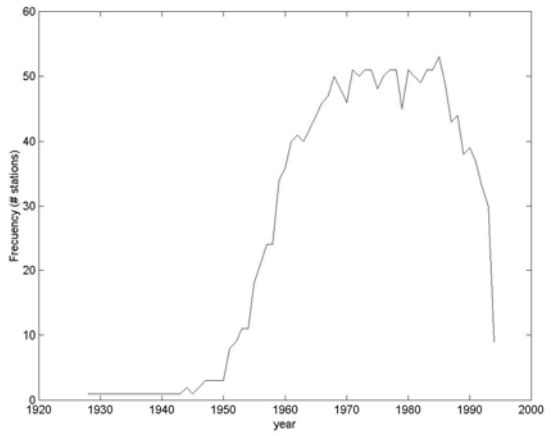

Fig. 5. For the SP of the annual cycle, frequency of stations with complete daily record versus year.

The mean SD of this dominant pattern is around 11-15/05 or pentad 27, but as Fig. 11a shows, there is a latitudinal variation of SD with early values in the South and late values in the North. The behavior of the SD pattern could be explained partially by the northward migration of the ITCZ that causes instability and humidity convergence in the region from boreal late spring to early autumn, mainly in the south of Central America (Figs. 9b-d and 10b-d), causing an increase in the deep convection that reduces the radiation and sunshine hours measured in the ground (Figs. 8a and c). Notice that in the beginning of the year both curves in Fig. 8a have a positive trend, but the values of R_t decrease after March, when the ITCZ began to get closer to the region. This is because most of the radiation was absorbed and reflected by cloud covertures (Fig. 8b), mainly in the southeast part of the region (Fig. 9b). During this period and the whole rainy season, trade winds are weaker (Fig. 7) than in the dry

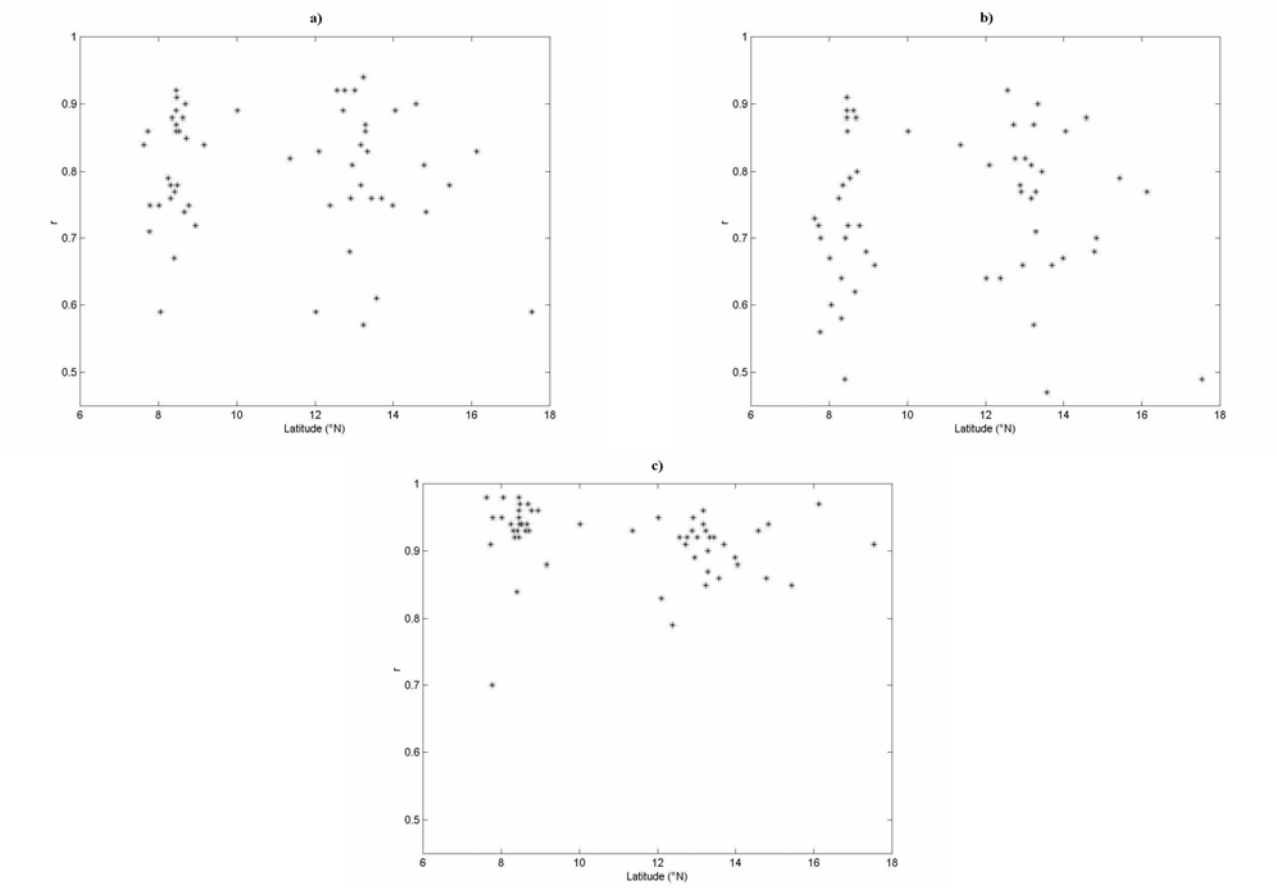

Fig. 6. For the SP of the annual cycle, correlations between: a) accumulates and days with precipitation, b) accumulates and consecutive days with precipitation and c) days with precipitation and consecutive days with precipitation, as a function of the latitude of the gauge station.

season and this allows the formation of mesoscale systems, such as sea breeze (Zárate, 1978), mostly in the Pacific side associated to deep convection. The frequency distribution of SD is shown in Fig. 12a, with a mode frequency having 25 cases. Some basic statistics of SD, ED and MSD calculation are in Table 2.

The first maximum of Fig. 4a appears in the middle of June (10-14/06 or pentad 33). As Fig. 9c shows, the migration of the ITCZ could not be the only reason for the generalized deep convection over the region during the rainy season (Figs. 9c to f), because normally the ITCZ is not found in latitudes higher than 10-12° N (Magaña *et al*., 1999), and there are values of OLR of less than 240 Wm^{-2} during the rainy season over the whole region that could be associated to deep convection (Cortez, 2000). Other factors that should be taken into account are the convergence of humidity (Fig. 10) and the LHF (Fig. 13), since these parameters increase during the rainy season

Table 2. Basic statistics of the SD, ED and MSD calculation. Values in parenthesis are the days associated to the pentad values described.

Statistic	**SD**	**ED**	**MSD**
N	90	90	78
Mean pentad	27.1 (11-15/05)	65.8 (17-21/11)	41.9 (20-24/07)
Standard Deviation	3.1	7.3	3.6
Pentad's Range	14	39	16
Mode	28 (16-20/05)	61 (28/10-01/11)	38 (05-09/07)
Median	28 (16-20/05)	65.5 (17-21/11)	42 (25-29/07)
Skewness	-0.313	1.263	0.774
Kurtosis	-0.268	2.112	0.295

Table 3. First eight wettest (driest) years for the four parts of the precipitation annual cycle described in the section 2. The columns 2, 3, 6 and 7 are the category for the SSTAs seasonal values in the Niño 3.4 and TNA indices of the corresponding seasons for those eight years and the columns 4 and 8 are the rank difference between these seasonal TNA and Niño 3.4 SSTAs. Values in parenthesis in column 1 are the Julian days that define the different parts of the annual cycle. The difference of the means, for the data in columns 4 and 8, has a *t* value of 6.6 which is significant at the 99.9%

	Wet				Dry		
FiP (97-153)							
Year	**Niño 3.4 category**	**TNA category**	**TNA-Niño 3.4 rank difference**	**Year**	**Niño 3.4 category**	**TNA category**	**TNA-Niño 3.4 rank difference**
1982	5	3	-44	1983	5	5	-3
1981	3	5	76	1975	1	1	-5
1966	4	5	22	1967	2	3	50
1970	4	5	33	1961	4	4	4
1968	2	3	24	1989	1	1	-1
1960	3	4	21	1955	1	3	61
1978	2	4	54	1965	3	2	-38
1979	4	5	24	1987	5	5	-11
SP (154-245)							
1988	1	5	132	1982	5	3	-70
1964	1	3	73	1991	5	1	-102
1973	1	4	89	1986	4	1	-67
1969	4	5	36	1976	3	1	-62
1981	1	4	74	1972	5	2	-103
1966	4	5	19	1965	5	3	-75
1960	3	4	32	1990	4	4	20
1968	4	2	-65	1975	1	1	20
TP (246-357)							
1975	1	1	13	1977	4	3	-42
1973	1	2	53	1987	5	5	5
1969	5	5	10	1976	5	3	-47
1955	1	5	129	1982	5	1	-120
1970	1	4	92	1972	5	2	-100
1971	1	2	15	1991	5	3	-72
1968	4	4	-12	1992	4	3	-33
1980	4	4	11	1986	5	1	-102
FoP (358-96)							
1970	5	5	27	1977	4	2	-63
1971	1	3	76	1992	5	3	-67
1963	3	5	77	1964	4	4	7
1960	3	4	35	1976	1	1	14
1978	4	4	5	1975	2	2	-9
1968	1	2	27	1973	5	2	-90
1981	2	5	71	1985	1	1	-3
1982	3	4	11	1994	4	1	-58

having a positive influence in convection over the region and also increasing evaporation and humidity advection.

Around the middle of July (15-19/07 that is, pentad 40, Fig. 4a), rainfall decreases. This period is known as *veranillo* or *canícula* and represents the MSD. Its frequency distribution is shown in Fig. 12b and its space distribution can be seen in Fig. 11b. There is some latitudinal variation in this parameter similar to the SD one, having early values mostly in the Southern-Pacific Slope and late values mostly in the Northern-Caribbean Slope. This behavior agrees with the description of Magaña *et al*. (1999) and Portig (1976). They found that MSD in the Pacific Slope of Central America occurs at earlier dates than the similar features found in some areas the Caribbean. The MSD mode frequency has 15 cases and the variance of this parameter was greater than the SD one (Table 2). During this month there is an increase in the radiation that reaches the ground (Fig. 8b) mainly in the Pacific slope mainly (Magaña *et al*., 1999). This aspect is not observed in the Fig. 9d, which shows even lower values of OLR than Fig. 9c. This could be a resolution problem of the data set that probably is mixing Pacific and Caribbean slope regimes. Even more, the presence of the low level jet in this month increases the humidity convergence near the Caribbean coast of Costa Rica (Amador, 1998; Amador *et al*., 2000) (Fig. 10d), in agreement with a trade winds increase in intensity during July (Fig. 7).

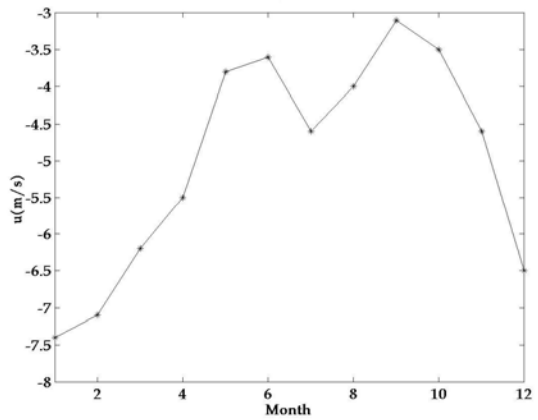

Fig. 7. Annual cycle for zonal wind component (u) at the 900 hPa level. Monthly values are from Juan Santamaría synoptic station (10° 00'N, 84° 12'W, from Alvarado, 1999), period used: 1972-1989). The u annual average value is –5 m s^{-1}. Notice that negative values are westward winds

Fig. 4a shows a second rainfall maximum in the middle of September (18-22/09 or pentad 53), that is wetter than the June one. This month also has high values of LHF in the north of the region and humidity convergence (Fig. 13e and 10e, respectively); low values of R_t, sunshine hours, OLR (Figs. 8a-c, and 9e, respectively); and weak trade winds (Fig. 7) in the whole region.

The mean ED value in Fig. 4a was located around 17-21/11 or pentad 65. The frequency distribution of this parameter is shown in Fig. 12c, with a mode frequency of 14 cases. Notice from Table 2 that, as for SD and MSD, the others central value parameters (mean and median) are similar, but having the largest variance ED. Fig. 11c, shows that early values were found mostly in the North Pacific and late values in the South. This latitudinal behavior of SD and ED is in agreement with the studies of Alfaro and Cid (1999b) that used only 37 Pacific slope stations and that of Cortez (2000) that used OLR data, and could be explained by the southward migration of the ITCZ and the decrease of the R^{TA} mainly, but the latest values were found in the North Caribbean Coast. These latest ED values require a deeper study having a different approach because they could be the incidence of cold fronts over the North-Caribbean Central American coast during the boreal winter. This is also supported by a zonal

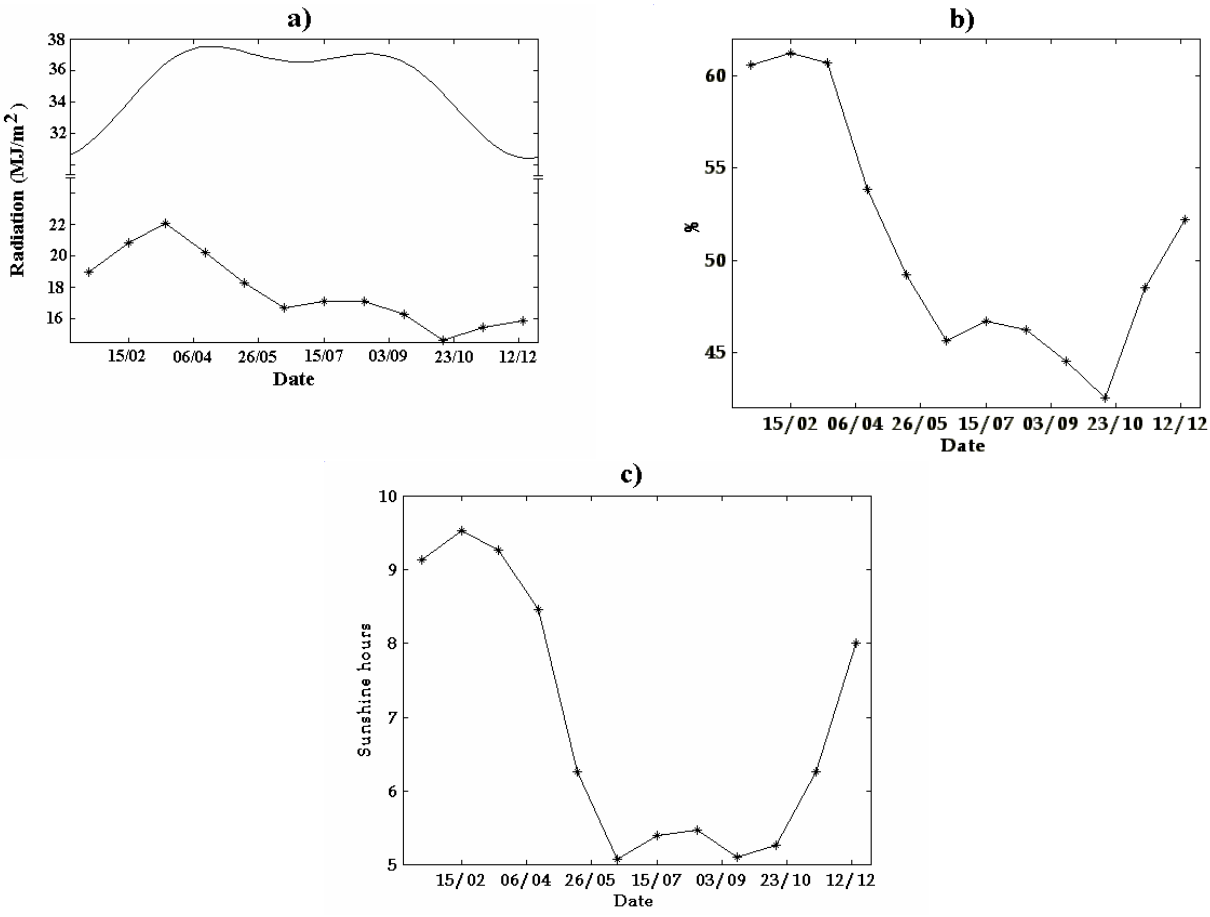

Fig. 8. a) Superior line is theoretical total radiation at the top of the atmosphere (R^{TA}) at the latitude of 10° 19', calculated as Rosemberg *et al.* (1983). The bottom line is the total radiation (R_t, direct plus diffuse) as the average of monthly climatic values of three Pacific slope stations: Fabio Baudrit (10° 01', 84° 16'), Liberia (10° 36', 85° 03') and Taboga (10° 21', 85° 09') (from Alfaro, 1993). b) R_t/R^{TA} ratio expressed as a percentage. c) Sunshine hours in the same three stations described in a).

Table 4. Correlations between the first three leading modes of the low filtered precipitation in Central America and the first three (six) non-ENSO unrotated (rotated) global SSTA modes defined by Enfield and Mestas-Nuñez (1999) and Mestas-Nuñez and Enfield (1999). Italic values are significant at the 95% level according to Ebisuzaki (1997).

		Central America Precipitation Modes		
		P1	**P2**	**P3**
	U1	-0.517	-0.053	-0.755
Global	**U2**	0.051	*-0.905*	-0.215
SST	**U3**	0.975	0.128	-0.07
Modes	**R1**	0.42	-0.225	*-0.842*
	R2	0.185	-0.332	*-0.814*
	R3	-0.947	0.067	-0.226
	R4	-0.404	-0.529	*-0.637*
	R5	0.618	-0.602	0.312
	R6	-0.293	-0.575	0.152

gradient of OLR and LHF over the region during January (Figs. 9a and 13a) with lower and higher values, respectively, associated to the Caribbean Coast.

Fig. 4b shows the next important regime that explains 8.0% of the total variance. This regime is associated to stations near the Caribbean coast of Honduras, Costa Rica and Panama (Fig. 4c). This regime was also noticed by Giannini *et al.* (2000). According to the criteria used by Enfield and Alfaro (1999), it is not possible to define a dry season using these stations. Also, the region around the Caribbean coast of Nicaragua, Costa Rica and Panama, has the lowest annual values of OLR. This rainfall mode shows a nearly homogeneous period between January and the middle of October, with accumulates typically between 30-50 mm by pentad (from pentad 2 to 56, this period is the 61.8% of the annual

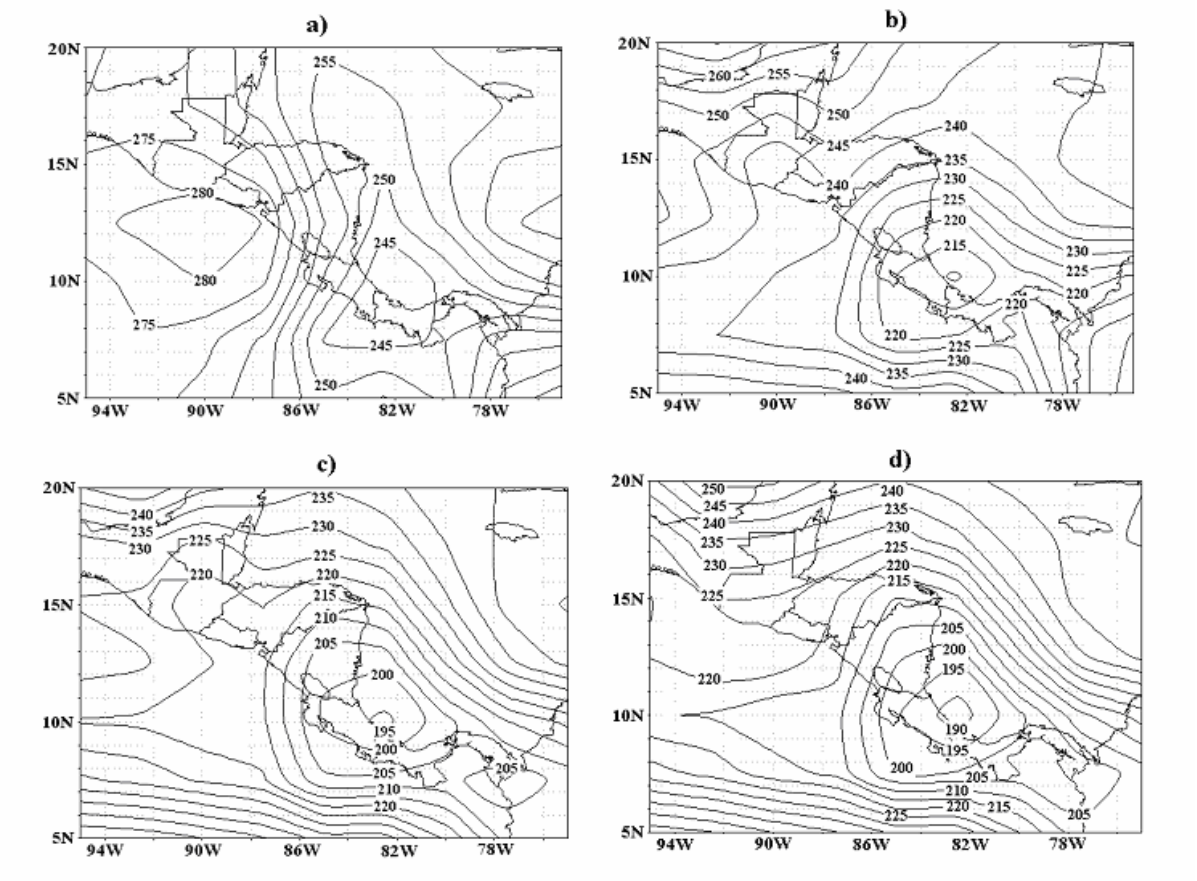

Fig. 9. OLR in Wm^{-2} for: a) January, b) May, c) June, d) July, e) September and f) November.

Table 5. Correlations between different tropical climate variability indices and the first three (six) non-ENSO unrotated (rotated) global SSTA modes defined by Enfield and Mestas-Nuñez (1999) and Mestas-Nuñez and Enfield (1999). Italic values are significant at the 95% level according to Ebisuzaki (1997). ENP and IAS are the indices for the eastern north Pacific and the Intra-Americas Sea West Hemisphere Warm Pool, respectively (Wang and Enfield, 2001).

		Climate Variability Indices								
		Niño 1&2	Niño 3	Niño 3.4	Niño 4	SOI	ENP	IAS	TNA	TSA
Global SST Modes	U1	0.559	*0.891*	*0.89*	*0.776*	*-0.913*	0.63	0.678	*0.766*	0.121
	U2	-0.495	0.168	0.338	0.486	-0.22	0.666	0.702	0.316	0.566
	U3	-0.656	-0.712	-0.491	-0.557	0.703	-0.672	-0.564	0.058	-0.655
	R1	-0.221	0.227	0.475	0.366	-0.262	0.239	0.39	*0.889*	-0.236
	R2	-0.13	0.445	*0.658*	0.54	-0.498	0.332	0.458	*0.804*	-0.191
	R3	*0.81*	*0.846*	0.636	0.6	*-0.831*	0.645	0.569	0.191	0.46
	R4	0.229	*0.856*	*0.957*	*0.954*	*-0.904*	*0.796*	*0.867*	*0.758*	0.304
	R5	*-0.804*	-0.438	-0.254	-0.117	0.47	-0.215	-0.138	-0.151	-0.14
	R6	-0.193	0.058	0.012	0.203	-0.096	0.68	0.582	-0.148	*0.954*

total). After that, there is a marked increase of the precipitation accumulation until the end of the year, showing a maximum in the beginning of December related with the humidity convergence by the end of the year in the Southeastern region (Fig. 10f). When this rainfall pattern is compared with the one plotted in Fig. 4a it is possible to see that the absolute minimum occurs in March for both curves, but the behavior during July is opposite, having a relative minimum in Fig. 4a and a relative maximum in Fig. 4b. This could be the result of two factors: the low level jet influence (Amador, 1998; Amador *et al*., 2000), and the topography-low level wind interaction which makes the Caribbean slope wetter than the Pacific slope during this part of the rainy season (Waylen *et al*., 1996), mainly by mechanic forcing caused by stronger trade winds. The precipitation mean annual accumulated by this regime is greater than the first one, with a value of 3214 mm and a range, given by one standard deviation (solid lines in Fig. 4b), of 1973-4455 mm.

3.2 Dry and wet precipitation seasons and their relationship with SSTAs in the tropical Atlantic and Pacific oceans

In the first (fifth) column of Table 3 are presented the first eight wettest (driest) years for the four parts of the precipitation annual cycle described in the section 2. Columns 2, 3, 6 and 7 are the category for the SSTAs seasonal values in the Niño 3.4 and TNA indices of the corresponding seasons for those eight years, and columns 4 and 8 are the rank difference between the seasonal TNA and Niño 3.4 SSTAs.

As the Table 3 shows, there was a non-clear category pattern from columns 2, 3, 6 and 7 for wet and dry years. Approximately 91% of the values in column 4 were positive. This means that during the wetter seasons, almost all the SSTAs seasonal values for the TNA were in an upper rank position than those of Niño 3.4 ones. From column 8, it is noted that 75% were negative. This means that SSTAs seasonal values for TNA tend to be in a lower rank position than those of Niño 3.4 ones during drier seasons. The results of Table 3 were partially suggested by the model found by Alfaro and Cid (1999a), which show stationary positive and negative relationships between the Central America PCPAs and the SSTAs of TNA/Niño 3 indices respectively. This suggests an upper (lower) SSTA rank TNA position than Niño 3 for wetter (drier) years. This idea is also supported by the result of Alfaro and Cid (1999b), Alfaro *et al.* (1998), and Enfield and Alfaro (1999), in which they noticed that the strongest rainfall response occurs when the TNA is in a configuration of meridional dipole (antisymmetric across the ITCZ) and the tropical Pacific is of opposite sign to the TNA. The rainy season in southern Central America tends to start early and end late in years that begin with warm SSTs in the tropical North Atlantic, and end dates are also delayed when the eastern equatorial Pacific is cool. Similar criteria and conclusions were obtained by Marengo *et al.* (2000), in their study of these aspects over the Brazilian Amazon Basin in South America.

These results could be explained by the studies of Taylor *et al.* (2001), Giannini *et al.* (2000), and Knaff (1997). They postulated that the main influence of the tropical eastern Pacific SSTAs is through a remote control by the maintenance in a southern position of the ITCZ during warm events. This is also in concordance with an increase of he pressure gradient to the equator that reinforces trade wind and also the vertical wind shear over the region. These issues increase the stability over the isthmus and do not favor deep convection processes. In other hand, the TNA influence is mainly by local forcing in which warmer conditions are associated with an increase of latent and sensible heat transfer to the overlaying troposphere. These conditions increase the humidity in low and middle levels, decreasing the pressure over the Caribbean region and favor the appearance of westerly wind anomalies across Central America in low level. This feature reinforces the establishment of mesoscale systems over the Pacific slope mainly, that are associated to deep convection (Zárate, 1978). During cold events in both oceans, the response of the atmosphere over the isthmus is normally opposite.

In spite that rank difference was negative in 1982

during FiP (column 4, Table 3), it was noticed that the difference in the rank between the TNA and tropical south Atlantic (TSA) were positive (not shown in Table 3) for the same season in 1982. This positive difference could be associated to a northern Atlantic ITCZ position and could decrease the meridional pressure gradient associated with weaker than average trade winds (Enfield, 1996; Giannini *et al.*, 2000). These weaker trade winds during FiP are associated with early SD because it allows the establishment of mesoscale systems (Alfaro and Cid, 1999b). Also, this could reflect the influence during 1982 of variability in a longer time scale than the interannual as noted by Mestas-Nuñez and Enfield (2001). Additionally, for most of the years in which that difference in column 8, Table 3, was positive (1990 and 1975 in SP, 1987 in TP and 1964 and 1976 in FoP), it was noted that difference in the rank between the TNA and TSA were negative. As we explained previously, this negative difference could be associated instead with an increase of the meridional pressure gradient related with stronger-than-average trade winds, working against the establishment of well defined mesoscale systems in the region. Those systems are responsible for most of the precipitation in the region year round (Zárate, 1978). Putting these two issues together, it is noted that approximately 91% of the dry years in Table 3 had negative values in the TNA-Niño 3.4 or TNA-TSA rank differences.

The ambiguous results with the use of indices category for the definition of wet and dry years was also found in previous works. Alfaro and Cid (1999b) found that longer rainy seasons were related to anomalous warm conditions in the TNA but it was noted that the condition in Niño 3 index could be both: warm or cool. Also they found that an early SD in the rainy season was dominated by warm conditions in Niño 3/TNA indices. This apparent paradox could be explained by the results of two of the recent works cited previously. Taylor *et al.* (2001) found positive correlation between the previous November-December-January SSTA for Niño 3 and February-March-April SSTA for TNA, and the precipitation in the Caribbean during FiP. As an explanation, Giannini *et al*. (2000) found that for the evolution of a warm ENSO phase, there is a spring weaker-than-average meridional SLP gradient between the North Atlantic subtropical high and the ITCZ, hence weaker-than-average easterly winds in the tropical latitudes of the north Atlantic that allows an early formation of mesoscale convective systems mainly on the Pacific slope of Central America.

Also, Taylor *et al*. (2001) found a negative correlation between August-September-October SSTA for Niño3 index and the precipitation for TP in the Caribbean. They postulated that equatorial Pacific can alter early rainfall season indirectly through its effects on the tropical Atlantic SST and can alter the late rainfall season due to their association with an altered vertical shear structure in the tropical structure of the tropical north Atlantic troposphere. This vertical shear is weaker-than-average during cold events in the eastern Pacific. This means that warm and cool SSTAs in the Niño3 index during the early and mid months of the year, respectively, could be related to longer rainy seasons in Central America because the tendency is for wet-than-average conditions when the convergent atmosphere flow dominates in the Caribbean during the rainy season preceding the mature phase of a cold ENSO event as is suggested by Giannini *et al*. (2000).

3.2 Relationships between the low-filtered Central American PCPAs and the tropical Atlantic and Pacific Oceans' decadal variability

Only the first three unrotated EOF PCPA modes of the low-filtered data showed some relationships with those global SSTs modes used for Enfield and Mestas-Nuñez (1999) and Mestas-Nuñez and Enfield (1999). These three precipitation modes explain 40.7, 28.0 and 14.3% of the variance, that is, around 83% of the total low filtered precipitation variance of the region. The modes' correlation is presented in Table 4. Fig. 14 shows the three PCPA modes and the three global SSTA modes that showed the main correlation with the first ones. The fraction's mean value between the low-filtered variance and the total non filtered variance for the grid point time series was 0.08. This is similar to the 0.09 value found for Air Surface Temperature in the region by Alfaro (2001).

In order to help the correct interpretation of the relationships between the precipitation EOF and the climatic variable, precipitation indices were calculated. They were the average of the grid points in which the explained variance associated to a particular EOF was maximum. The correlation coefficient between the index and the EOF was then calculated. All of them were negative. This means that a positive (negative) correlation between any PCPA mode and any SSTA mode means a negative (positive) correlation between the correspondent PCPA index and the same SSTA mode.

The first precipitation mode, P1, has high positive and negative correlations with U3, the Atlantic multidecadal variability, and R3, the eastern tropical Pacific interdecadal variability, respectively. U3, appears to be related to the 500 hPa pressure height mid-tropospheric pattern of the Artic Oscillation/North Atlantic Oscillation (AO/NAO), and R3 captures interdecadal STTA changes in the eastern tropical Pacific that modulate the interannual ENSO. These SSTA changes induce changes in the equatorial Walker circulation that force westward winds in the central equatorial Pacific (Enfield and Mestas-Nuñez, 1999; Mestas-Nuñez and Enfield, 1999).

Table 5 shows the correlations between some low-filtered climate variability indices that are related with climate variability in Central America (e.g., Wang and Enfield, 2001; Enfield, 1996; and Waylen *et al*., 1996), and the SSTA unrotated and rotated modes. The time period used to calculate the correlations was the same of the low filtered precipitation time series (1963-1994), which differs from the time period used in the Table 2 of

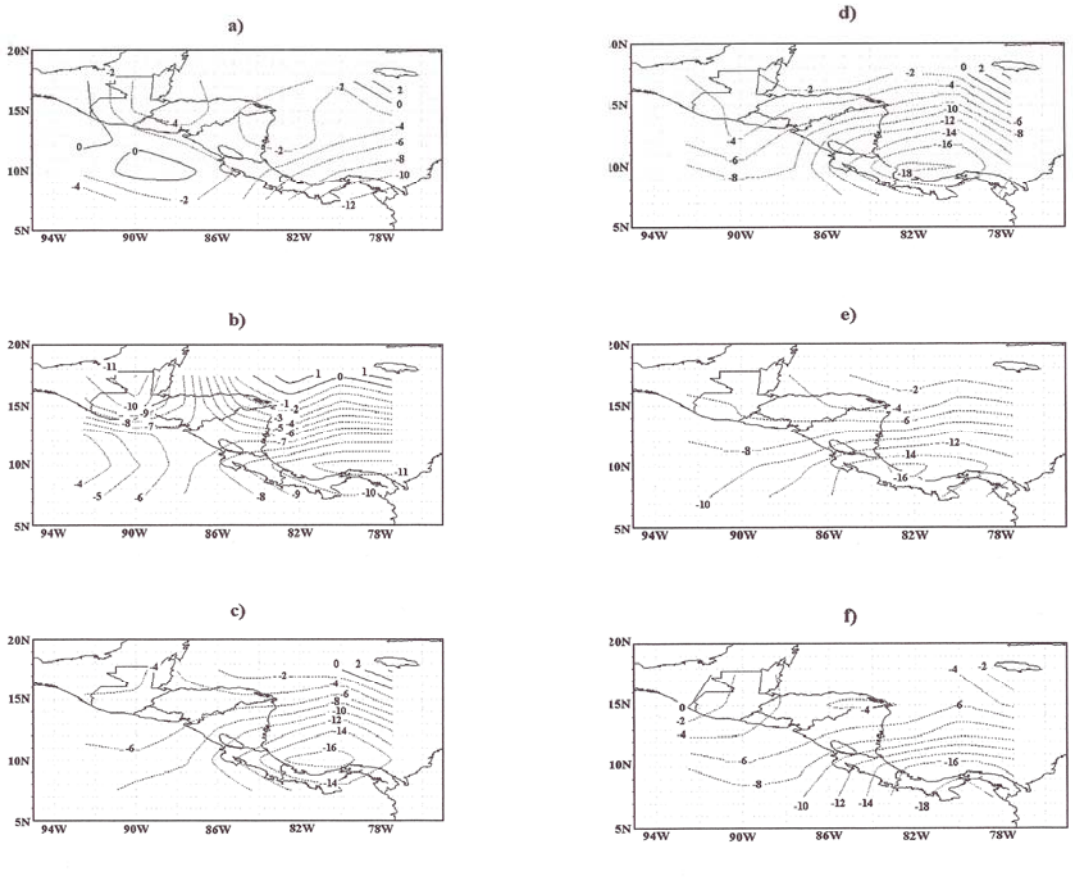

Fig. 10. Divergence of humidity, ($\tilde{\mathbf{N}} \times (q\mathbf{V})$) * 10^8 in s^{-1}, for: a) January, b) May, c) June, d) July, e) September and f) November. Negative values means convergence.

Mestas-Nuñez and Enfield (2001). From Table 5, we noted that U3 (R3) has a negative (positive) correlation with SSTA indices in the Eastern Pacific (Niño 1&2, Niño 3 and ENP), and also a positive (negative) correlation with SOI. There is also a negative correlation between U3 and R3 (see Table 3 in Mestas-Nuñez and Enfield 1999). So, both indices influence the precipitation in Central America in a similar way of the described by Mestas-Nuñez and Enfield (2001) for the low-pass component of Niño 3 region. They described that on decadal scales, the ENSO and the residual variability show similar patterns for SST, SLP and surface wind stress, but the tropospheric direct circulation responds quite differently. They found, on decadal scales, that variability in Niño 3 region is associated with convergence (divergence) in the 850 hPa wind field and with divergence (convergence) in the 200 hPa wind field over Central America during warm (cold) events. That behaviour is in favour or against the deep convection in the region during warm or cold decadal events, respectively.

The second precipitation mode, P2, has a high negative and significant correlation with U2, the Pacific multidecadal variability (Table 4). This SSTA mode is related with the 500 hPa pressure height mid tropospheric pattern of the North Pacific (NP) (Enfield and Mestas Nuñez, 1999). As Table 5 shows, U2 has positive correlations with the indices of the West Hemisphere Warm Pool (WHWP) in the tropical eastern north Pacific and in the Intra-Americas Sea (ENP and IAS, respectively, according to Wang and Enfield, 2001). These correlations could associate bigger or smaller-than average WHWP to processes that work in favour or against the precipitation in Central America, respectively (Knaff, 1997), because they are associated with lower or higher than average SLP in the Caribbean that cause relative convergence or divergence in low troposphere level (Giannini *et al.,* 2000).

According to Table 4, the third mode, P3, show significant and negative correlations with R1, the North Atlantic multidecadal variability, R2, the Eastern North Pacific interdecadal variability, R4, the Central tropical

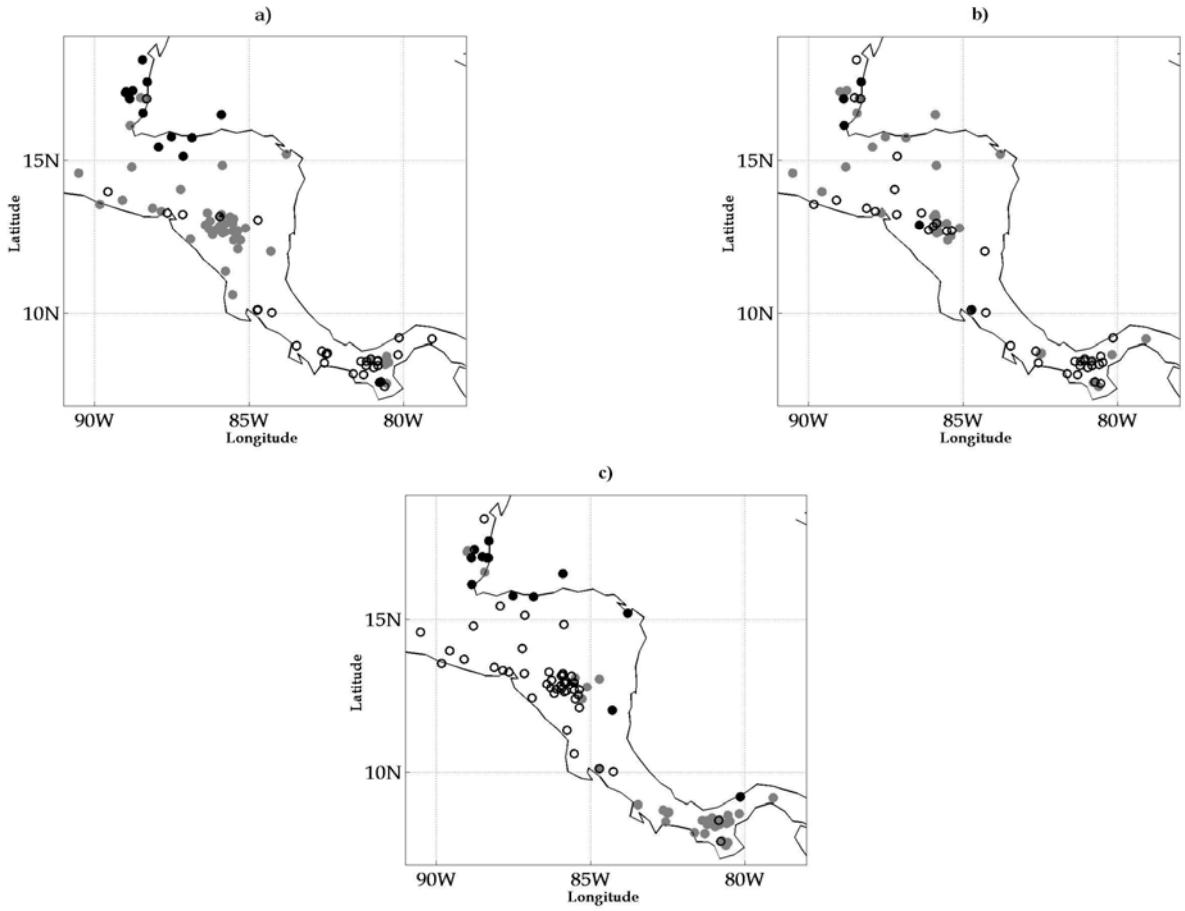

Fig. 11. Spatial distribution of a) SD, open circles are pentad values lesser than 27 (dates before 11/05), gray filled circles are pentad values between 27 and 29 (dates between 11-25/05) and black solid circles are values greater than 29 (dates after 25/05), b) MSD, open circles are pentad values lesser than 42 (dates before 25/07), gray filled circles are pentad values between 42 and 46 (dates between 25/07 and 18/08) and black solid circles are values greater than 46 (dates after 18/08), and c) ED, open circles are pentad values lesser than 64 (dates before 11/11), gray filled circles are pentad values between 64 and 71 (dates between 11/11 and 21/12) and black solid circles are values greater than 71 (dates after 21/12).

Pacific interdecadal variability and also with U1, the Pacific interdecadal variability. Mestas-Nuñez and Enfield (1999) summarized that R1 captures multidecadal fluctuations in the North Atlantic consistent with local atmospheric forcing related to the NAO. R2 captures interdecadal fluctuations in the eastern North Pacific related to local atmospheric forcing through surface fluxes and upwelling along the coast of North America, and R4 captures different aspects of the Pacific interdecadal variability related to the PDO and that is consistent with local atmospheric forcing. Meanwhile, the U1 mode is associated with the 500 hPa pressure height mid tropospheric pattern of the Pacific North American (PNA).

It is noted in Table 5 that modes U1, R4 and in a less degree R2, have positive correlations with the different eastern and central tropical Pacific indices, so, their influence over precipitation in decadal scales for P3 is very similar to that described for P1 in which warm or cold SSTA events are in favour or against the deep convection in the region, respectively. Additionally, U1, R1, R2 and R4 have high positive correlations with the SSTA variability in the TNA and IAS. This means that in decadal scales warm or cold SSTA events in TNA are in favour or against the deep convection in the region, respectively. This agrees with the results of Goldenberg *et al.* (2001) that show a high positive correlation between the SSTA variability in the North Atlantic and the TNA that act in concert with the overlying tropical troposphere circulation, such that warmer (colder) SSTA correspond to reduced (increased) vertical wind shear over the TNA. This issue reinforce (decrease) the convection over the Caribbean region and is associated with seasons of more (less)-than-average number of hurricanes.

The P1 correlation with modes U3 and R3 also agree with the high positive (0.86) correlation between P1 and the difference of the smoothed indices TNA and Niño 3, and P3 correlation with modes R1 and U1, agree with the negative and significant correlation between P3 and the smoothed indices TNA and Niño 3.4 (–0.85 and –0.60, respectively, not shown in Table 5). There is a positive

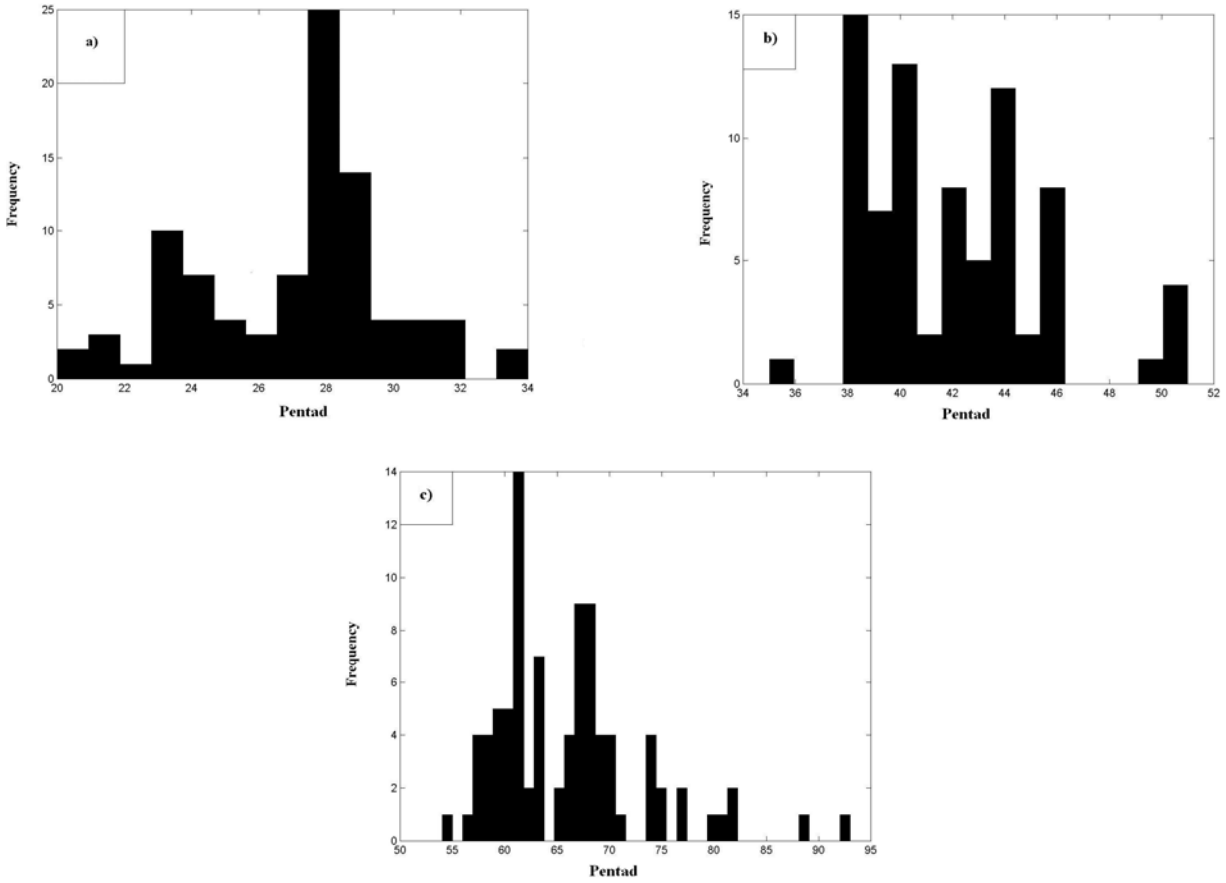

Fig. 12. Frequency distribution for: a) SD, b) MSD and c) ED.

correlation between the variability in the North Atlantic and the TNA region (Goldenberg *et al*., 2001) and also between the smoothed Niño 3-Niño3.4 and the R3-PNA pattern (Mestas-Nuñez and Enfield, 2001).

4. Conclusions

By means of a simple analysis it was possible to calculate the SD, MSD and ED, which are important intraseasonal aspects of the dominant annual rainfall cycle in Central America, having an associated time scale of less than a month. There is a latitudinal dependence in the SD and ED. For SD, early values were found mostly in the Southern region and late values in the Northern region. For ED the behavior was opposite. This could be explained partially by the seasonal migration of the ITCZ that is associated with instability and humidity convergence over the region during the rainy season, by the annual cycle of the trade winds that are strong during the winter and weaker from the middle spring to late autumn, and also by the annual cycle of the R^{TA} that has the highest values over the region during the rainy season that favors the LHF mostly in the North. The latitudinal pattern for the MSD was similar to the SD one but is less defined, in which the influence of the sea basin is apparently important.

Wetter regimes were found in the Caribbean coast that also showed the lowest values of OLR around the year, with a minimum near Nicaragua, Costa Rica and Panama. This is related to a mixture of high humidity convergence and topographic-wind effects. Related to this regime is the low level jet in the Caribbean during the summer in which an increase in the eastern zonal wind is associated to important humidity convergence near the Nicaragua and Costa Rica coast. This factor is not present during January in which the eastern zonal wind, in low troposphere level, presents the strongest values in the region.

It was noticed that drier (wetter)-than-average periods in Central America were in general dominated by an upper (lower) eastern tropical Pacific rank positions than the TNA SSTAs. This is because the climate variations of the Caribbean and Central America depend on the troposphere structure over this region, and the seasonal march, depend on the interaction of SSTs variability in both the Atlantic and Pacific as Enfield and Alfaro (1999) explain. So, as these authors reported before, a conclusion is that oppositely signed SSTAs in Niño 3.4 and TNA are associated with enhanced rainfall departures over the Caribbean and Central America, and an expanded rainy (contracted dry season) over lower Central America. Similar conclusion about this "seesaw"

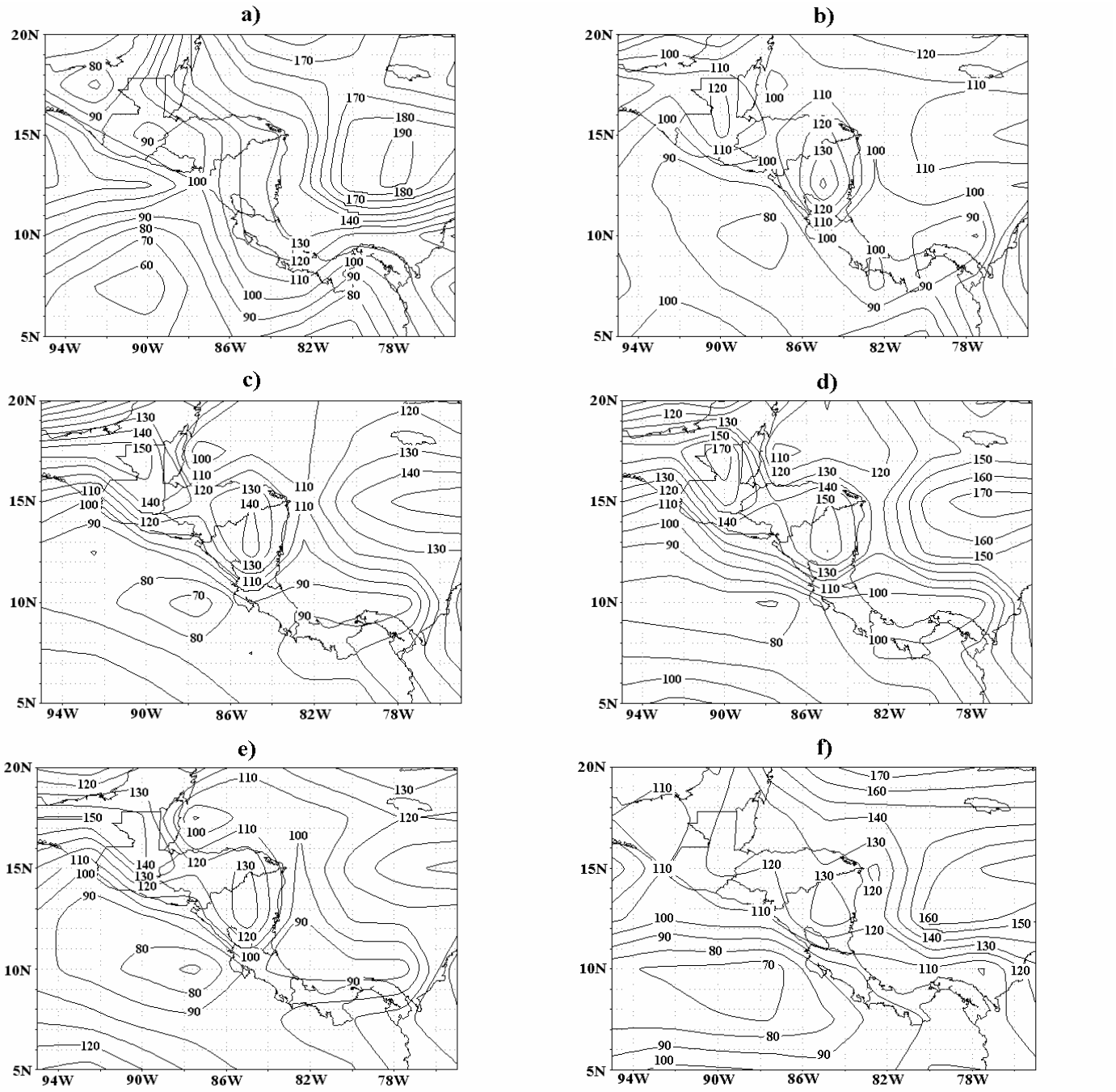

Fig. 13. LHF in Wm^{-2} for: a) January, b) May, c) June, d) July, e) September and f) November.

in the SST field was also noticed by Giannini *et al.* (2000) for the SLP field.

The cases that are described previously respond generally to linear studies between SSTAs and PCPAs. However, the atmosphere over Central America responds to influences of both oceans and other external forcings that are not considered in this analysis as a whole. This response is far from being linear and the comparation of the SSTAs influence in the overlaying atmosphere, from TNA and Niño 3 for example, not easy. An example of this situation is the wetter conditions in the region during the TP of the rainy season of 1969. In this year both oceans had warm conditions during the TP, with SSTAs in the fifth category in spite that its rank difference was also positive (see Table 3).

Another factor that should be taken in account and that increases the complexity of the problem, is that variation of precipitation in Central America responds in different ways to external forcing from time scales such as intraseasonal, interannual and interdecadal. Related to this last time scale, precipitation showed positive correlations with decadal SSTA variability in the TNA and in the

eastern tropical Pacific. The modulation of the TNA in this time scales is very similar to what is proposed for the interannual scale. For the Niño 3 it is opposite, showing that warm (cold) events are associated with convergence (divergence) in low levels over Central America and divergence (convergence) in high levels. This flow pattern could be associated to processes that work in favor (against) the deep convection over the region.

Acknowledgments.

This work was supported by Task2, CRN-TC3 (038)-IAI and by VI 112-99-305, 805-94-204, 805-98-506, Universidad de Costa Rica grants. The author thanks to Dr. Víctor Magaña, CCA, UNAM, México, for the monthly grid rainfall data set as a collaboration from CRN 073-IAI, and to Dr. Jorge Amador, School of Physics-CIGEFI, University of Costa Rica, for his useful discussions during this study. Also to Dr. Javier Soley, School of Physics-CIGEFI, University of Costa Rica, and Dr. David Enfield, NOAA-AOML, for their help with analysis routines and the SSTAs data. Finally, to Dr. Walter Fernández, School of Physics-CIGEFI, University of Costa Rica, for his manuscript's comments.

RESUMEN

Usando 94 estaciones pluviométricas de registro diario, se calcularon los ciclos anuales promedio dominantes en la región centroamericana por medio del análisis de funciones ortogonales empíricas. Esto permitió estimar aspectos importantes del ciclo anual tales como el inicio y término de la estación lluviosa así como el período de veranillo o canícula, notándose una variación latitudinal de los mismos. Se encontró que la región está dominada por un ciclo anual promedio que captura cerca del 72% de la varianza. Este ciclo anual está explicado por una combinación de sistemas y parámetros que involucran la migración latitudinal de la ZCIT, la variación estacional de la radiación solar, que influye sobre el flujo de calor latente, y el viento en bajo nivel y su interacción con la orografía, principalmente. El segundo ciclo anual en importancia explica sólo el 8% de la varianza en la región. Este dominó en estaciones ubicadas sobre la costa Caribe de Honduras, Costa Rica y Panamá. La precipitación en Centroamérica presentó relaciones distintas con los océanos Atlántico y Pacífico tropical en las escalas interanuales y decadales. En la escala interanual, los años más húmedos (secos) en la región estuvieron relacionados en general con anomalías de la temperatura superficial del mar más cálidas (frías) en el Atlántico Tropical que en el Pacífico Tropical Este. Mientras que en la escala interdecadal la precipitación mostró correlaciones positivas con ambas regiones oceánicas tropicales.

References

Alfaro, E., 2000: Response of Air Surface Temperatures over Central America to Oceanic Climate Variability Indices. *Tópicos Meteorológicos y Oceanográficos*, **7**(2), 63-72

Alfaro, E., 1993. Algunos aspectos del clima en Costa Rica y su relación con fenómenos de escala sinóptica y planetaria. Degree Thesis in Meteorology, School of Physics, University of Costa Rica, San José, Costa Rica. 75pp.

Alfaro, E. y L. Cid, 1999a: Ajuste de un modelo VARMA para los campos de anomalías de precipitación en Centroamérica y los índices de los océanos Pacífico y Atlántico Tropical. *Atmósfera*, **12**(4), 205-222.

Alfaro, E. y L. Cid, 1999b. Análisis de las anomalías en el inicio y el término de la estación lluviosa en Centroamérica y su relación con los océanos Pacífico y Atlántico Tropical. *Tóp. Meteor. Oceanog.,* **6**(1), 1-13.

Alfaro, E., L. Cid and D. Enfield, 1998. Relaciones entre el inicio y el término de la estación lluviosa en Centroamérica y los Océanos Pacífico y Atlántico Tropical. *Investigaciones Marinas*, 26, 59-69.

Alvarado, L., 1999. Alteración de la atmósfera libre sobre Costa Rica durante eventos de El Niño. Degree Thesis in Meteorology, School of Physics, University of Costa Rica, San José, Costa Rica. 187pp.

Amador, J., V. Magaña and J. Peréz, 2000. The low level jet and convective activity in the Caribbean. In: Abstracts of the 24th Conference on Hurricanes and Tropical Meteorology. American Meteorological Society. Fort Lauderdale, Florida. 29 May - 2 June. 114-115.

Amador, J., 1998. A climate feature of the tropical Americas: The trade wind easterly jet. *Tóp. Meteor. Oceanog*, **5**(2), 91-102.

Cortez, M., 2000. Variaciones intraestacionales de la actividad convectiva en México y América Central. *Atmósfera*, **13** (2), 95-108.

Ebisuzaki, W., 1997. A method to estimate the statistical significance of a correlation when the data are serially correlated. *J. Climate*, **10**, 2147-2153.

Enfield, D., 1996. Relationships of inter-American rainfall to tropical Atlantic and Pacific SST variability. *Geophys.Res. Lett.*, **23**, 3305-3308.

Enfield, D. and A. Mestas-Nuñez, 1999. Multiscale variabilities in global sea surface temperatures and their relationships with tropospheric climate patters. *J. Climate*, **12**, 2719-2733.

Enfield, D. and E. Alfaro, 1999. The dependence of Caribbean rainfall on the interaction of the tropical Atlantic and Pacific Oceans. *J. Climate*, **12**, 2093-2103.

Giannini, A., Y. Kushnir and M. Cane, 2000. Interannual variability of Caribbean rainfall, ENSO and the Atlantic Ocean. *J. Climate*, **13**, 297-311.

Goldenberg, S., C. Landsea, A. Mestas-Nuñez and W. Gray, 2001. The recent increase in Atlantic hurricane activity: Causes and Implications. *Science*, **293**, 474-479.

Knaff, J., 1997. Implications of summertime sea level pressure anomalies in the tropical Atlantic region. *J. Climate*, **10**, 789-804.

Magaña, V., J. Amador and S. Medina, 1999. The mid-summer drought over Mexico and Central America. *J. Climate*, **12**, 1577-1588.

Marengo, J., B. Liebmann, V. Kousky, N. Filizola and I. Wainer, 2001. Onset and end of the rainy season in the Brazilian Amazon Basin. *J. Climate,* **14**, 833-852.

Mestas-Nuñez, A. and D. Enfield, 2001. Eastern Equatorial Pacific SST variability: ENSO and non-ENSO components and their climatic associations. *J. Climate*, **14**, 391-402.

Mestas-Nuñez, A. and D. Enfield, 1999. Rotated global modes of non-ENSO sea surface temperature variability. *J. Climate*, **12**, 2734-2746.

Porting, W. 1976. The climate of Central America, p. 405-478. *In* W. Schweidtfeger (ed.). World Survey of Climatology, Vol. 12: Climates of Central and South America. Elsevier, Nueva York.

Rosemberg, N., B. Blad and S. Verna, 1983. *Microclimate: The Biological Environment*. 2 ed. John Wiley & Sons, 495p.

Soley, F., 1994. Suavizamiento de series cronológicas geofísicas con ruido blanco y rojo aditivo. *Revista Geofísica*, **41**, 33-58.

Taylor, M., D. Enfield and A. Chen, 2002. Influence of the tropical Atlantic versus the tropical Pacific on the Caribbean rainfall. Journal of Geophysical Research, 107(C9).

Wang, C. and D. Enfield, 2001. The tropical Western Hemisphere warm pool. *Geophys. Res. Lett.*, **28**(8), 1635-1638.

Waylen, P., C. Caviedes and M. Quesada, 1996. Interannual variability of monthly precipitation in Costa Rica. *J. Climate*, **9**, 2606-2613.

Zárate, 1978. Comportamiento del viento en Costa Rica. Nota de Investigación N° 2. Instituto Meteorológico Nacional, San José, Costa Rica, 30pp.